Microfluidic radiolabeling of biomolecules with PET radiometals

Dexing Zeng [a], Amit V. Desai [b], David Ranganathan [a], Tobias D. Wheeler [b], Paul J.A. Kenis [b], David E. Reichert [a],*

[a] Radiological Sciences Division, Mallinckrodt Institute of Radiology, Washington University School of Medicine, 510 South Kingshighway Blvd., St. Louis, MO 63110, USA
[b] Department of Chemical & Biomolecular Engineering, University of Illinois at Urbana-Champaign, Urbana, IL 61801, USA

A R T I C L E   I N F O

A B S T R A C T

Introduction: A robust, versatile and compact microreactor has been designed, fabricated and tested for the labeling of bifunctional chelate conjugated biomolecules (BFC-BM) with PET radiometals.
Methods: The developed microreactor was used to radiolabel a chelate, either 1,4,7,10-Tetraazacyclodode-cane-1,4,7,10-tetraacetic acid (DOTA) or 1,4,7-triazacyclononane-1,4,7-triacetic acid (NOTA) that had been conjugated to cyclo(Arg-Gly-Asp-DPhe-Lys) peptide, with both ^{64}Cu and ^{68}Ga respectively. The microreactor radiolabeling conditions were optimized by varying temperature, concentration and residence time.
Results: Direct comparisons between the microreactor approach and conventional methods showed improved labeling yields and increased reproducibility with the microreactor under identical labeling conditions, due to enhanced mass and heat transfer at the microscale. More importantly, over 90% radiolabeling yields (incorporation of radiometal) were achieved with a 1:1 stoichiometry of bifunctional chelate biomolecule conjugate (BFC-BM) to radiometal in the microreactor, which potentially obviates extensive chromatographic purification that is typically required to remove the large excess of unlabeled biomolecule in radioligands prepared using conventional methods. Moreover, higher yields for radiolabeling of DOTA-functionalized BSA protein (Bovine Serum Albumin) were observed with ^{64}Cu/^{68}Ga using the microreactor, which demonstrates the ability to label both small and large molecules.
Conclusions: A robust, reliable, compact microreactor capable of chelating radiometals with common chelates has been developed and validated. Based on our radiolabeling results, the reported microfluidic approach overall outperforms conventional radiosynthetic methods, and is a promising technology for the radiometal labeling of commonly utilized BFC-BM in aqueous solutions.

© 2013 Elsevier Inc. All rights reserved.

1. Introduction

Over the past decade, interest in the use of radiolabeled peptides for use in positron emission tomography (PET) imaging for preclinical development and clinical diagnostics, and radiation-based therapeutics has increased. Such agents are becoming more prevalent since many peptide-targeted receptors are overexpressed in cancer, and the development of routine methods of solid-phase peptide synthesis has allowed the development of highly specific imaging probes and/or therapeutic agents with the appropriate choice of PET radioisotope [1]. These agents are generally composed of two parts, the biomolecule (BM) responsible for receptor targeting and a bifunctional chelate (BFC) for coordinating the radioisotope.

The cyclic pentapeptide cyclo($-$Arg-Gly-Asp-(D)-Phe-Lys-) (cyclo(RGDfK)) is a highly potent and selective inhibitor for the $\alpha_v\beta_3$ receptor, an integrin required for tumor-induced angiogenesis, and is over-expressed in various types of tumors [2]. Many radioligands containing the peptide sequence of cyclo(RGDfK) have been

prepared to monitor expression of the $\alpha_v\beta_3$ receptor, and their evaluations have been carried out in both murine tumour models [3–5] and patient studies [5,6], with promising results. The preparation of these radioligands requires that cyclo(RGDfK) peptides be labeled with positron-emitting radionuclide such as ^{18}F, ^{64}Cu or ^{68}Ga. Among these PET radioisotopes, the distribution of ^{18}F is limited to relatively small distances from the production cyclotron facility, due to the short half-life of ^{18}F ($t_{1/2} = 1.83$ hr). On the other hand, ^{64}Cu and ^{68}Ga allow for wider distribution, either due to relatively long half life ($t_{1/2} = 12.7$ hr for ^{64}Cu) or availability of an on-site, self-contained generator (^{68}Ge/^{68}Ga generator for ^{68}Ga), which has drawn increased attention to ^{64}Cu and ^{68}Ga as promising radionuclides [7–13]. ^{64}Cu can be effectively produced by both reactor-based and accelerator-based methods, and has suitable decay characteristics ($\beta+$: 0.653 MeV, 17.4%; $\beta-$: 0.578 MeV; 39%) that allow this radiometal to be used as a PET imaging agent [10–12], and a nuclear therapy agent [12,14,15]. ^{68}Ga is a positron emitter with a half-life of 67.6 min and decays via positron emission (89%), and its relatively shorter half-life and hydrophilic nature are beneficial for the rapid renal clearance of small peptides labeled with ^{68}Ga. In addition, ^{68}Ga can be conveniently and economically obtained from the ^{68}Ge/^{68}Ga

* Corresponding author. Tel.: +1 314 362 8461; fax: +1 314 362 9940.
E-mail address: ReichertD@wustl.edu (D.E. Reichert).

generator, and the long half-life of the parent nuclide ^{68}Ge ($t_{1/2}$ = 280 days) allows PET imaging on-site without the need for a dedicated cyclotron [16]. The ready availability of ^{68}Ga for clinical PET has prompted rapid tracer development based on this isotope, and more than 40 centers in Europe have utilized this type of generator, with most of them focusing on either basic or transitional research on radiochemistry of ^{68}Ga [12].

Although widely used conventional methods for labeling with radiometals suffer from several limitations. Due to the radiation emitted by PET radionuclides, the radiolabelings are typically carried out in a heavily lead-shielded fume hood or bunker to minimize radiation exposure to the radiochemists. In addition, radiosyntheses are usually carried out at very low mass amounts (usually less than a few hundred nanograms) of radioactive material. To facilitate convenient handling and efficient mixing, the tiny amounts of radioisotopes need to be dissolved in a relatively large amount of solvent, which results in nanomolar concentrations of the radiometals [17,18]. To compensate for the slow reaction kinetics resulting from such low concentrations, a very large (~100-fold) excess of the non-radioactive precursor (biomolecule conjugate) is used to promote rapid and efficient incorporation of the radioisotope into the PET imaging agent. However, with such a large stoichiometric excess of precursor, issues such as radioisotope pre-concentration (prior to reaction), side reactions (due to possibly more reactive minor impurities), product purification and product analysis can be problematic. To achieve high specific activities using conventional labeling techniques, careful control over reaction conditions and extensive chromatographic purification are required to separate the radiolabeled compounds from the cold precursors. To address the above issues associated with conventional radiosynthesis, we have developed compact microreactors for rapid, efficient labeling without the need for using large excess reagents.

Microfluidic devices, comprising enclosed micro-channels (normally 10–500 μm wide or tall), mixing units, heaters, pumping systems, are able to control and process chemical or biological reactions in a continuous flow manner or batch mode [19–22]. When used for radiolabeling biomolecules, microreactors can potentially circumvent many of the existing limitations [23–26]. Microfluidic radiolabeling offers: (1) the ability to manipulate small volumes, which mitigates issues associated with dilution effects; (2) efficient mixing which greatly improves reaction kinetics; (3) the ability for fine level of control over reaction conditions, such as concentrations, temperature, enabling reliable and reproducible labeling; and (4) a much smaller overall footprint of the system, which drastically reduces the volume that requires shielding.

Most microfluidic approaches for the synthesis of radiopharmaceuticals have focused primarily on the synthesis of ^{18}F- and ^{11}C-labeled agents [22,27,28]. For example, Lee et al. [28] developed a poly(dimethylsiloxane) (PDMS)-based microreactor for the multistep synthesis of ^{18}F-FDG, a radiotracer commonly used to detect cancer *via* PET. An improved version of this microreactor provided yields of 96% after ~15 min of total synthesis time, compared to 75% yield after ~45 min using an automated apparatus for conventional synthesis [29]. However, an off-chip purification step was still required to obtain a radiochemical purity of ~99%, and loss of ^{18}F through reaction with or absorption by the PDMS was noted as a significant issue. In other work, Lu et al. [30] developed a hydrodynamically-driven microreactor and investigated the effect of infusion rate on the yields of several ^{18}F and/or ^{11}C-labeled carboxylic esters using a T-junction, flow-through glass microfluidic system. They observed that incomplete diffusive mixing at lower residence times adversely affected the yield. Recently, our group has developed PDMS-based microreactors for labeling BFC-BM with radiometals [31]. These microreactors were validated with radiosynthesis of ^{64}Cu labeled RGD peptide, and demonstrated higher yields compared to conventional techniques under identical reaction conditions. Following up on the validation

with ^{64}Cu labeling, we report here the versatility of this microreactor-based method by utilizing two commonly used PET radiometals, ^{64}Cu and ^{68}Ga, to label two common bifunctional chelates, DOTA and NOTA (more specifically S-2-(4-Isothiocyanatobenzyl)-NOTA (p-SCN-Bn-NOTA)), conjugated to a clinically relevant biomolecule, the pentapeptide *cyclo*(RGDfK). We present a direct comparison between radiolabeling performance of the microreactor and conventional methods, and results on optimization of the labeling conditions using the microreactor.

2. Experimental procedures

2.1. General

A 50 mCi ^{68}Ge/^{68}Ga generator was obtained from Eckert & Ziegler EUROTOPE GmbH. A Hewlett Packard model 1050 high-performance liquid chromatography (HPLC) apparatus was used for purifying synthesized and labeled compounds. The luna HPLC column and Strata X-C column were purchased from Phenomenex. Mass spectra were obtained with an Waters LC-MS API-3000 spectrometer. Three sets of female 1/4-28 to female Luer lock adaptors with ferrules and nuts, PEEK tubing of 1/16″ OD and 0.01″ ID, and a NanoTight kit with 1/16″×0.027″ FEP sleeves, obtained from Upchurch Scientific (Oak Harbor, WA) and Microbore PTFE tubing (0.012″ ID×0.030″ OD) obtained from Cole-Parmer (Vernon Hills, IL) were assembled to connect syringes to the microreactor. The 75 mm×50 mm×1 mm glass slide, used to assemble the microreactor, and the Fisher Vortex Genie 2 were obtained from Fisher Scientific (Pittsburgh, PA). Test grade, 3″ silicon wafers, obtained from University Wafer (South Boston, MA) were used to fabricate SU-8 molds for the microreactor. Three microliter flow modular pump components, which included a syringe pump, a pump driver circuit, and a power supply, were obtained from Harvard Apparatus (Holliston, MA). The Kapton-insulated, 2″×2″, thin film heater, the Omega CN740 temperature controller, and an Omega SA 1-RTD probe were obtained from Omega Engineering (Stamford, CT). The Harrick plasma cleaner was obtained from Harrick Plasma (Ithaca, NY). Eppendorf tubes were obtained from MIDSCI, Inc. (St. Louis, MO). The BioScan AR-2000 radio-TLC plate reader was purchased from Bioscan, Inc. (Washington, DC). The Thermomixer was obtained from Eppendorf North America (Hauppauge, NY). Millipore Centriplus Centrifugal Concentrator (2 mL, 3000 NMWL) was obtained from Millipore (Billerica, MA). TLC-silica gel [SG] plates were obtained from Whatman Thin Layer Chromatography (Piscataway, NJ), and iTLC-silica gel [SG] was purchased from Gelman. Gas-tight, microliter syringes were obtained from Hamilton Co. (Reno, NV). The Capintec CRC-712 M radioisotope dose calibrator used to measure activities for retention experiments was obtained from Capintec, Inc. (Ramsey, NJ).

All solvents and reagents were purchased from commercial sources and used without further purification. DOTA-NHS-ester and S-2-(4-Isothiocyanatobenzyl)-NOTA (p-SCN-Bn-NOTA) were purchased from Macrocyclics (Dallas, TX). Bovine serum albumin (BSA protein), 3-[4-(2-Hydroxyethyl)-1-piperazinyl]propanesulfonic acid (HEPPS), ammonia acetate, acetonitrile and trifluoroacetic acid (TFA) were purchased from Sigma-Aldrich (St. Louis, MO). *Cyclo*(RGDfK) was purchased from Peptides International, Inc. (Louisville, KY). De-ionized water (DI-H$_2$O) was produced using a Millipore Milli-Q water system. RTV 615 poly(dimethyl siloxane) (PDMS) was obtained from General Electric Company (Waterford, NY). SU-8 2050 was obtained from MicroChem Corporation (Newton, MA). (Tridecafluoro-1,1,2,2-tetrahydrooctyl) trichlorosilane was obtained from Gelest, Inc. (Morrisville, PA). ^{64}Cu^{2+} was produced at Washington University School of Medicine, and was obtained in 0.1 M HCl solution. 6 mL of 0.1 M HCl was used to flush ^{68}Ga^{3+} (from the ^{68}Ge/^{68}Ga generator) onto Strata X-C column, and then ~20 mCi of ^{68}Ga^{3+} was recovered by eluting with 1.0 mL of 0.02 M HCl, 98% Acetone.

2.1.1. Fabrication and operation of the microreactor

The PDMS-based microreactor for labeling BFC–BMs with radio-metals was fabricated as described previously [31], and is comprised of three major components (Fig. 1A): (1) a staggered herringbone [32] mixing channel to passively mix reagents; (2) a series of incubation reservoirs for the radiometal–ligand mixture and (3) a thin-film heater for heating the mixture. The radiometal and buffer solutions are pumped into the microreactor through inlets 1 and 2, respectively, and then flowed through the mixing channel. As the two solutions flowed along the microchannel, they mix by chaotic advection induced by the geometry of the herringbones. After the buffer and radiometal mixture arrive at the end of the first mixing channel, the biomolecule conjugate (BFC-BM) solution is pumped into the microreactor through inlet 3 and mixed with the radio-metal-buffer mixture in a second mixing microchannel with staggered herringbone grooves defined in the ceiling. The mixed reagents then fill a series of five hexagonal reservoirs (holding tanks), and flow is stopped. The mixture is heated to the desired temperature and allowed to react for a specified residence time which is two minutes less than the actual reaction time thereby accounting for the two minutes it takes for reactant introduction and product flushing. After the previously set residence time, buffer solution was pumped into the microreactor to flush the product out, through outlet 1. Fig. 1B shows a diagram of the configuration used to operate the microreactor. The flow of each reagent stream; radiometal, buffer, and ligand, into the microreactor was driven by syringe pumps controlled by a LabVIEW virtual instrument (VI). Communication between the VI and the syringe pump drivers was facilitated through a serial connection. The VI was used to set the individual flow rates and regulate the timing of the pumps, with inputs for controlling the incubation time, the total flow rate, the desired volume of product (the maximum being the total volume of the reservoirs, ~50 μL), and the stoichiometric molar ratios of buffer : radiometal and ligand : radiometal. For radiolabeling at elevated temperatures, a thin-film heater, placed in contact with the glass surface of the microreactor, was used to heat the microreactor, and a temperature controller and resistance temperature detector (RTD) probe were used to maintain the temperature within ±1 °C of the desired temperature set-point. The radiometal syringe pump, heater, and microreactor were shielded on four sides and below with 2″ of lead shielding. The radiometal syringe was fitted with a 7.5 cm length of PEEK tubing connected to an Upchurch Luer lock fitting. The PDMS microreactor was fit with a 10 cm length of PTFE tubing connected to an Upchurch NanoTite fitting. The syringe and PEEK "needle" were inserted into the fitting and tightened.

2.1.2. Synthesis and purification of NOTA-cyclo(RGDfK)

To a mixture of 6.03 mg cyclo(RGDfK) and 8.26 mg p-SCN-Bz-NOTA (1.2 equiv.) in 0.5 mL dimethylformamide (DMF), 1.0 mL of 0.1 M sodium bicarbonate was added, and then the mixture was allowed to react overnight at room temperature in the dark (Scheme 1A). The crude NOTA-cyclo(RGDfK) was then purified on a Waters HPLC system using an Alltech Econosil C18 semi-preparative column RP18 (10 μm, 4.6×250 mm) with a mobile phase of 10 vol% acetonitrile and 90 vol% de-ionized water with 0.1 vol% trifluoroacetic acid (TFA), at a flow rate of 3.0 mL/min. Under these conditions, the NOTA-cyclo(RGDfK) was eluted at 11.5 min. The pooled NOTA-cyclo(RGDfK) fractions were lyophilised overnight, and white powder was obtained as a pure product. The identity and purity of the purified NOTA-cyclo(RGDfK) peptide were confirmed by LC-MS using an Phenomenex Luna C18(2) column (5 mm, 4.6×150 mm). The analysis was performed using the following gradient of 0.1 v% TFA in de-ionized water (A) and 0.1 vol% TFA in acetonitrile (B) with a flow rate of 0.5 mL/min: 0–5 min: 90% A, 10% B; 5–20 min: 10% A, 90% B; 20–24 min: 10% A, 90% B; 25–30 min: 90% A, 10% B. A UV chromatogram and a TIC chromatogram are shown in Fig. 2A. The mass spectrum of the peak at ~14.6 min is shown in Fig. 2B, and verified that the peak corresponds to pure NOTA-cyclo(RGDfK), with m/z, $[M+H]^+ = 1054.7$.

2.1.3. Preparation of NOTA-cyclo(RGDfK) stock solution

Stock solutions of 1.0 mM NOTA-cyclo(RGDfK) were prepared by dissolving 5.28 mg of purified DOTA-cyclo(RGDfK) in 500 μL of a mixture of 10 mM NH_4OAc (pH=4.50) and acetonitrile (MeCN) (80:20 v%), and then diluting these solutions with 10 mM NH_4OAc (pH=4.50) to give final concentrations of 200, 100, 40, and 2 μM NOTA-cyclo(RGDfK).

2.1.4. Synthesis and purification of DOTA-cyclo(RGDfK)

A mixture of 6.03 mg cyclo(RGDfK), 8.38 mg DOTA-NHS (1.1 equiv.) and 14.0 μL triethylamine (TEA) (10 equiv.) in 1.0 mL DMF was allowed to react overnight at room temperature in the dark (Scheme 1B), then 3 mL of DI-H₂O were added and stirred for another 30 min to hydrolyze the excess DOTA-NHS ester. The crude DOTA-cyclo(RGDfK) was then purified on a Waters HPLC system using an Alltech Econosil C18 semi-preparative column RP18 (10 μm, 4.6×250 mm) with a mobile phase of 15 vol% acetonitrile and 85 vol% de-ionized water with 0.1 vol% TFA, at a flow rate of 3.0 mL/min. Under these conditions, the NOTA-cyclo(RGDfK) eluted at 13.5 min. The pooled DOTA-cyclo(RGDfK) fractions were lyophilised overnight, and white powder was obtained as a pure product. The identity and purity of the purified DOTA-cyclo (RGDfK) peptide were confirmed by LC-MS using an Phenomenex
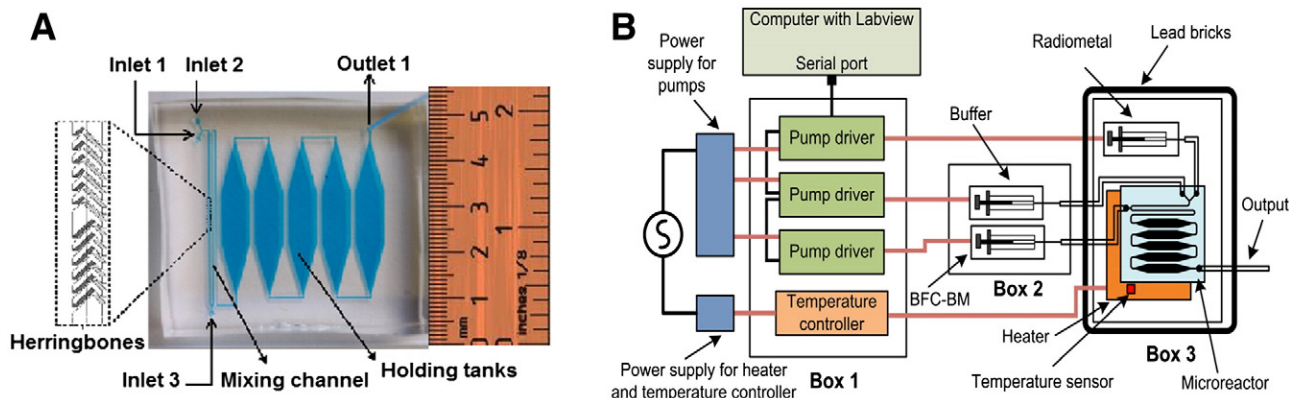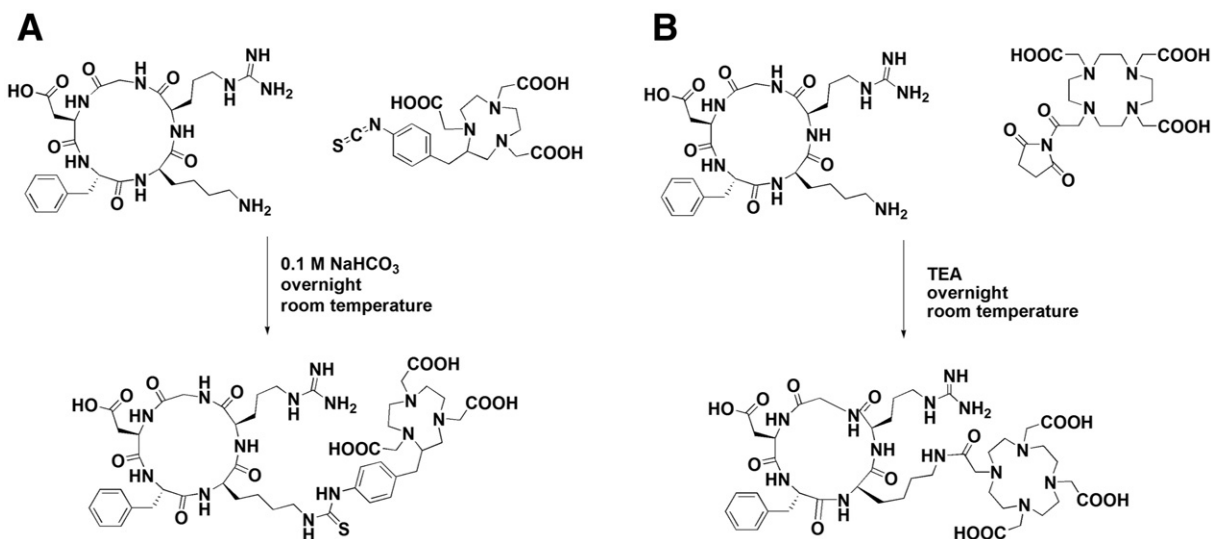

Fig. 1. (A) Optical micrograph of the microreactor and (B) schematic of the microreactor system for radiolabeling (1b). The mixing channels and incubation reservoirs are filled with blue dye. The length, width, and height of the PDMS portion of the microreactor are ~2.0″×~2.0″×~0.25″.

Scheme 1. Synthesis of NOTA-*cyclo*(RGDfK) (A) and DOTA-*cyclo*(RGDfK) (B).

Luna C18(2) column (5 mm, 4.6×150 mm), consistent with the previously reported data [31].

2.1.5. Preparation of DOTA-cyclo(RGDfK) stock solution

Stock solutions of 1.0 mM DOTA-*cyclo*(RGDfK) were prepared by dissolving 4.96 mg of purified DOTA-*cyclo*(RGDfK) in 500 μL of a mixture of 10 mM NH4OAc (pH = 6.8) and acetonitrile (MeCN)
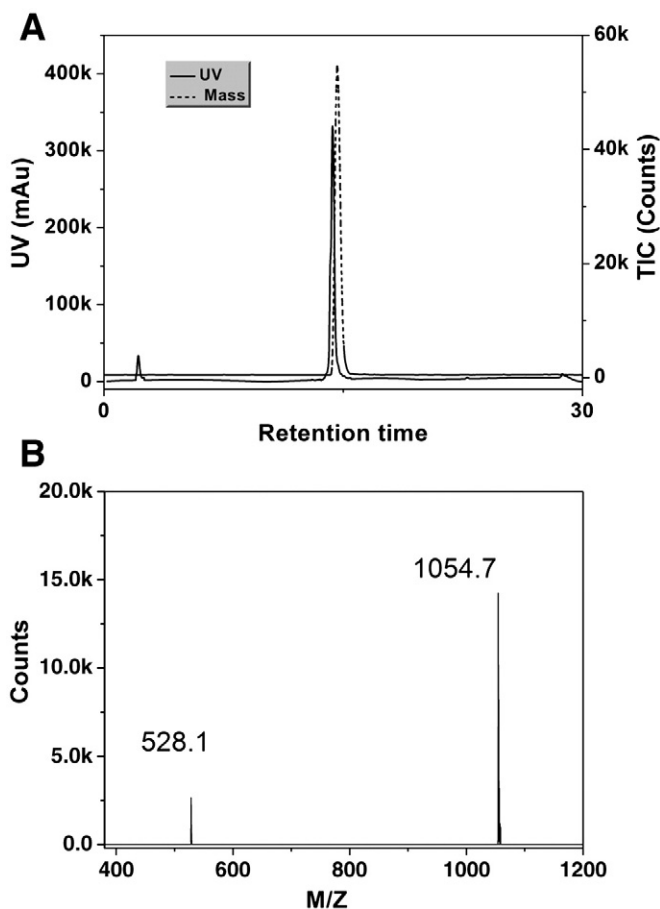

Fig. 2. Purity of NOTA-cyclo(RGDfK), as indicated by (A) UV (solid line) and Mass (TIC, dashed line) traces of LC-MS chromatograms. (B) The mass spectrum of the material corresponding to the peak with an elution time of 14.6 min in (A).

(80:20 vol%), and then diluting these solutions with 10 mM NH4OAc (pH = 6.8) to give final concentrations of 200, 100, 40, and 2 μM DOTA-*cyclo*(RGDfK).

2.1.6. Preparation of 200 μM DOTA conjugated BSA protein (DOTA-BSA)

To a solution of 2.68 mg BSA protein in 1.80 mL PBS buffer (10 mM, pH = ~8.50), 306 μg DOTA-NHS in 200 μL DMSO was added. After the pH was adjusted to ~9.50 by addition of 1.0 M Na3PO4, the mixture was incubated for 2 h at room temperature. Then, the mixture was concentrated to 200 μL with 5-kDa molecular weight cutoff ultrafiltration membrane centrifugal filter devices (Millipore). The residue was diluted with 1.80 mL NH4OAc buffer (10 mM, pH = ~6.80), and then concentrated to 100 μL; this sequence was repeated an additional 5 times. The pure DOTA-BSA was obtained in 200 uL of NH4OAc buffer (10 mM, pH = ~6.80), and then was diluted with 200 uL of NH4OAc buffer (10 mM, pH = ~6.80) to give the final concentrations of 200 μM DOTA-BSA, which was stored in −20 °C freezer. The number of DOTA moieties on each BSA protein was determined to be 4 using a published method [33].

2.1.7. Preparation of no-carrier added $^{68}Ga^{3+}$ and carrier-added $^{68}Ga^{3+}$ stock solution

The 1.0 mL $^{68}Ga^{3+}$ (~20 mCi, in 0.02 M HCl, 98% Acetone) was dried, and the residue was re-dissolved in 2.0 mL of 1.0 M HEPES bufffer (pH = 4.50) to give the no-carrier-added $^{68}Ga^{3+}$ stock solution with specific activity of 10 μCi/μL (decay corrected).

Various carrier-added Gallium solutions were prepared from this no-carrier-added stock solution. 200 μM carrier-added $^{68}Ga^{3+}$ solution was prepared by mixing 100 μL $^{68}Ga^{3+}$ solution (10 μCi/μL) with 20 μL of 10 mM non-radioactive Gallium solution and 880 μL of 1.0 M HEPES bufffer (pH = 4.50). The carrier-added $^{68}Ga^{3+}$ solutions with different concentrations were obtained by the dilution of the above 200 μM carrier-added $^{68}Ga^{3+}$ solution with 1.0 M HEPES bufffer (pH = 4.50).

2.1.8. Preparation of no-carrier added $^{64}Cu^{2+}$ and carrier-added $^{64}Cu^{2+}$ stock solution

The cyclotron-produced $^{64}Cu^{2+}$ (5 mCi, in 0.1 M HCl) was diluted with 10 mM NH4OAc (pH = 6.50) to obtain the no-carrier added $^{64}Cu^{2+}$ stock solution with specific activity of 10 μCi μL^{-1}. Various carrier-added copper solutions with different concentrations were then prepared from this no-carrier-added stock solution. 200 μM carrier-added $^{64}Cu^{2+}$ solution was prepared by mixing 100 μL $^{64}Cu^{2+}$ solution (10 μCi μL^{-1}) with 20 μL of 10 mM non-radioactive copper

solution and 880μL of 10 mM NH$_4$OAc (pH = 6.50). The carrier-added ^{64}Cu^{2+} solutions with different concentrations were obtained by the dilution of the above 200μM carrier-added ^{64}Cu^{2+} solution with 10 mM NH$_4$OAc (pH = 6.50).

2.1.9. Measurement of retention of ^{68}Ga^{3+}

Before use in retention measurements, the fabricated microreactors were cleaned with 1.0 mL of 1 N nitric acid to remove trace amount of metals, and then flushed with 5 mL of 10 mM NH$_4$OAc buffer solution (pH = 4.50).

2.1.9.1. Pre-treatment with Ga^{3+}/Na$^+$. 100μL of 10 mM NaCl/GaCl$_3$ solution was injected into the microchannel and allowed to sit for 30 min. The microchannel was then flushed with 5 mL of 10 mM NH$_4$OAc buffer solution (pH = 4.50).

2.1.9.2. Retention measurement. 30μL of no-carrier added ^{68}Ga^{3+} in 10 mM NH$_4$OAc buffer solution (pH = 4.50) was injected into the microchannel. After 10 min, the ^{68}Ga^{3+} solution was displaced from the microchannel by 1.0 mL of air, *via* syringe. The microchannel was then flushed with 1.0 mL of 10 mM NH$_4$OAc buffer (pH = 4.50). The percent of injected activity retained in the microchannel was calculated from the known activity of the injected solution, and the difference between the activity left behind in the microchannel after flushing and the initial activity of the microchannel measured before the ^{68}Ga^{3+} solution was injected, all measured with the Capintec radioisotope dose calibrator.

2.1.10. Measurement of retention of ^{64}Cu^{2+}

Before using in retention mesurements, the fabricated microreactors were cleaned with 1.0 mL of 1 N nitric acid to remove trace

metals, and then flushed with 5 mL of 10 mM NH$_4$OAc buffer solution (pH = 4.50).

2.1.10.1. Pre-treatment with Cu^{2+}. 100μL of a 10 mM CuCl$_2$ solution was injected into the microchannel and allowed to sit for 30 min. The microchannel was then flushed with 5 mL of 10 mM NH$_4$OAc buffer solution (pH = 4.50).

2.1.10.2. Retention measurement. 30μL of no-carrier added (only radioactive) ^{64}Cu^{2+} in 1.0 M HEPES bufffer (pH = 4.50) was injected into the microchannel. After 10 min, the ^{64}Cu^{2+} solution was displaced from the microchannel by 1.0 mL of air, *via* syringe. The microchannel was then flushed with 1.0 mL of 10 mM NH$_4$OAc buffer (pH = 4.50). The percent of injected activity retained in the microchannel was calculated from the known activity of the injected solution, and the difference between the activity left behind in the microchannel after flushing and the initial activity of the microchannel measured before the ^{64}Cu^{2+} solution was injected, were all measured with the Capintec radioisotope dose calibrator.

2.1.11. Conventional radiolabeling of the DOTA-cyclo(RGDfK)/NOTA-cyclo(RGDfK) with ^{64}Cu^{2+}

30μL of 100μM DOTA-*cyclo*(RGDfK)/NOTA-*cyclo*(RGDfK) solution was firstly added to 15μL of 10 mM NH$_4$OAc (pH = 6.50) in a 1.6 mL Eppendorf tube. 60μL of 50μM ^{64}Cu^{2+} solution (in 10 mM NH$_4$OAc, pH = 6.50) was then added to the mixture. The mixture was vortexed for 10 s, and incubated in Eppendorf thermomixer for 12 min at a temperature of 23, 37 or 47°C (Scheme 2A and 2B). The final concentration of ^{64}Cu^{2+} and NOTA-*cyclo*(RGDfK)/DOTA-*cyclo*(RGDfK) was 28.6μM in both methods.
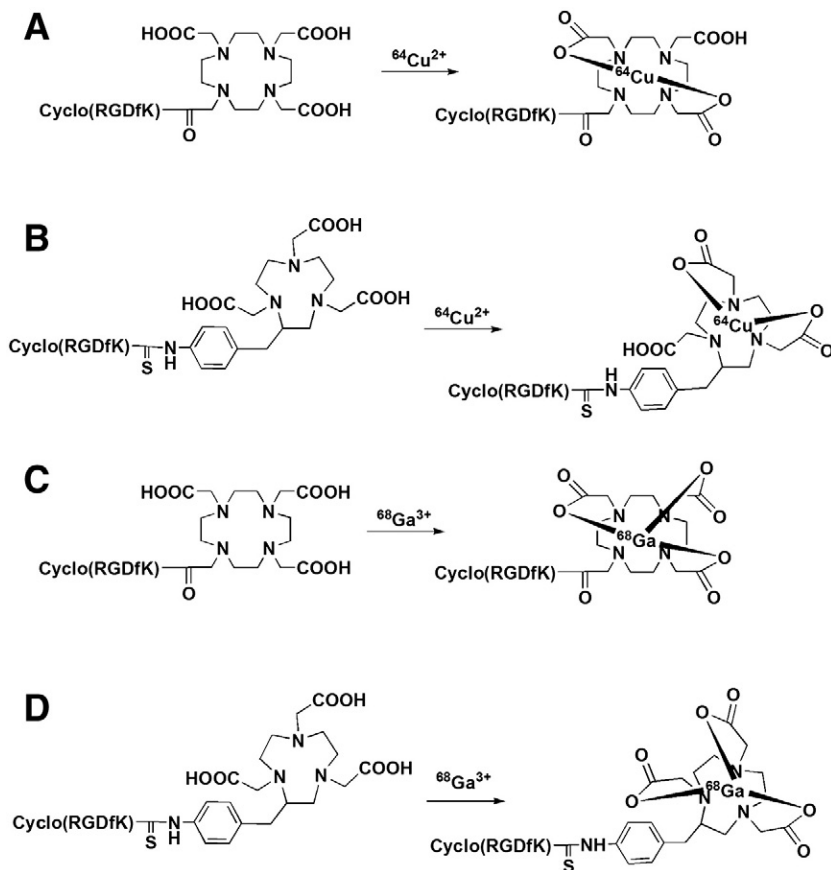
Scheme 2. Radiolabeling of DOTA-*cyclo*(RGDfK) with ^{64}Cu (A); NOTA-*cyclo*(RGDfK) with ^{64}Cu (B); DOTA-*cyclo*(RGDfK) with 68 Ga (C); NOTA-*cyclo*(RGDfK) with 68 Ga (D).

2.1.12. Conventional radiolabeling of DOTA-cyclo(RGDfK)/NOTA-cyclo(RGDfK) with $^{68}Ga^{3+}$

30 μL of 100 μM DOTA-cyclo(RGDfK)/NOTA-cyclo(RGDfK) solution was added to 15 μL of 10 mM NH$_4$OAc (pH = 4.50) in a 1.6 mL Eppendorf tube. 60 μL of 50 μM $^{68}Ga^{3+}$ solution (in 1.0 M HEPES buffer, pH = 4.50) was then added to the mixture. The mixture was vortexed for 10 s, and incubated in Eppendorf thermomixer for 12 min at a temperature of 23, 37 or 47 °C (Scheme 2C and 2D). The final concentration of $^{68}Ga^{3+}$ and NOTA-cyclo(RGDfK)/DOTA-cyclo(RGDfK) was 28.6 μM in both methods. The labeling results were analyzed by radio-HPLC and/or iTLC(SG).

2.1.13. Conventional labeling of DOTA-BSA with $^{64}Cu^{2+}$/$^{68}Ga^{3+}$

10 μL of 100 μM DOTA-BSA solution was mixed to 5 μL of 10 mM NH$_4$OAc (pH = 6.50 for ^{64}Cu, pH = 4.50 for ^{68}Ga) in a 1.6 mL Eppendorf tube. 50 picomoles (10 μL of 5.0 μM ^{68}Ga, 50 μL of 1.0 μM ^{64}Cu) of the above no-carrier added radiometal stock solution (BSA to M = 20:1) was then added to the mixture. The mixture was vortexed for 10 s, and then incubated in Eppendorf thermomixer for 22 min at a temperature of 37 °C. The labeling results were analyzed by radio-FPLC and/or iTLC(SG). The concentration of the no-carrier added radiometal was caculated based on its E.S.A. as reported [34,35].

2.1.14. Microreactor radiolabeling procedure

The microreactor is operated as previously described in *Fabrication and operation of the microreactor* section. For the radiolabeling experiments summarized in Fig. 5A (*effect of residence time on extent of reaction*) and Fig. 5B (*effect of mixing method and temperature on extent of reaction*), the following solutions were used: (1) 50 μM carrier-added $^{68}Ga^{3+}$/$^{64}Cu^{2+}$ solution, (2) 100 μM NOTA-cyclo(RGDfK)/DOTA-cyclo(RGDfK) stock solution, and (3) 10 mM NH$_4$OAc (pH = 6.8 for ^{64}Cu, and pH = 4.50 for ^{68}Ga) buffer. Using the LabVIEW interface, the pumps were programmed to combine the radiometal (1), ligand (2), and buffer (3) solutions with the same volumetric ratios as those used for the conventional radiolabeling procedure, giving a ligand-to-metal molar ratio of 1:1 and a final concentration of carried-added radiometal and BFC-BM of 28.6 μM. The total flow rate was set to 25 μL/min, the total volume was set to 25 μL. An additional 25 μL of buffer was pumped into the microreactor to fill all the reservoirs. For the experiments in Fig. 6A, the temperature was set to 37 °C, and the residence time was set to 5, 10, and 20 min (resulting in total reaction times, t_{REA} = 7, 12, and 22 min: *e.g.*, 1 min for filling + 10 min for residence + 1 min for flushing). For the experiments in Fig. 6B, the residence time was set to 10 min (t_{REA} = 12 min), and the temperature was set to 23, 37 and 47 °C. After the collection of product, the yield of radiolabeling raction was determined as described in the *Measurement of radiolabeling yield* section.

For the radiolabeling experiments summarized in Fig. 5 (*effect of concentration on extent of reaction*), combinations of stock solutions and buffer-to-metal molar ratio inputs were used to give the following final concentrations of radiometal and ligand (1:1 molar ratio): 1 μM (2 μM stock solutions, 1:1 buffer-to-radiometal ratio), 10 μM (40 μM stock solutions, 500:1 buffer-to-radiometal ratio), 20 μM (40 μM stock solutions, 1:1 buffer-to-radiometal ratio), 30 μM (100 μM stock solutions, 130:1 buffer-to-radiometal ratio), 50 μM (100 μM stock solutions, 1:1 buffer-to-radiometal ratio), and 90 μM (200 μM stock solutions, 11:1 buffer-to-radiometal ratio). Experiments were performed with the same settings as listed above, a residence time of 10 min (t_{REA} = 12 min) and at a temperature of 37 °C. After the collection of product, the yield of radiolabeling raction was determined as described below in the *Measurement of radiolabeling yield* section.

For the radiolabeling experiments summarized in Figs. 7 & 8 (*label the DOTA-BSA protein with no-carrier added radiometals: $^{68}Ga^{3+}$/$^{64}Cu^{2+}$*): 100 μM ligand (DOTA-BSA), 10 mM NH4OAc buffer (pH =

6.50 for ^{64}Cu, and pH = 4.50 for ^{68}Ga), 1:1 buffer-to-radiometal ratio and 20: 1 ligand-to-radiometal ratio. Experiments were performed with the same settings as listed above, and with t_{RES} = 22 and 32 min and at a temperature of 37 °C. After the collection of product, 1.0 μL of 50 mM EDTA solution (pH = 5.00) was added and the mixture was incubated for a minute to chelate with unreacted radiometals. Then, the yield of radiolabeling reaction was determined as described below in *Measurement of radiolabeling yield* section.

Throughout the course of radiolabeling experiments, three trial runs were performed before data was recorded to ensure proper functioning of the microreactor after syringe pump or heater settings were changed and after depleted syringes were replenished.

2.1.15. Measurement of radiolabeling yield

In the case of the ^{64}Cu labeling of NOTA/DOTA conjugated cyclo(RGDfK), at the end of each reaction run, 1.0 μL aliquot of product was spotted onto a TLC(SG) plate and developed using a mobile phase of methanol/10% ammonium formate buffer (2:1 volume ratio). After developing, the radio-TLC plates were then counted using the Bioscan radio-TLC scanner to quantify free and bound $^{64}Cu^{2+}$. The radiolabeling yields were calculated by dividing the area of the radioactivity peak obtained for the bound $^{64}Cu^{2+}$ by the total area of the radioactivity peaks obtained for both bound and free $^{64}Cu^{2+}$.

For the ^{68}Ga labeling of NOTA/DOTA conjugated cyclo(RGDfK), at the end of each reaction run, a 2.0 μL aliquot of product was spotted onto a iTLC(SG) plate and developed using 0.1 M citric acid as the mobile phase. After developing, the iTLC plates were then counted using the Bioscan radio-TLC scanner to quantify free and bound $^{68}Ga^{3+}$. The radiolabeling yields were calculated by dividing the area of the radioactivity peak obtained for the bound $^{68}Ga^{3+}$ by the total area of the radioactivity peaks obtained for both bound and free $^{68}Ga^{3+}$.

For the ^{64}Cu/^{68}Ga labeling of DOTA-BSA, after challenging with EDTA, a 2.0 μL aliquot was spotted onto a iTLC(SG) plate and developed using a mobile phase of methanol/10% ammonium formate buffer (2:1 volume ratio). After developing, the iTLC plates were then counted using the Bioscan radio-TLC scanner to quantify free and bound radiometal. The radiolabeling yields were calculated by dividing the area of the radioactivity peak obtained for the bound radiometal by the total area of the radioactivity peaks obtained for both bound and free radiometal.

3. Results and discussion

As mentioned previously, the microfludic approach employed in this work provides several advantages as discussed above, leading to overall better performance in the radiolabeling of biomolecules compared to conventional methods. In the following sections, the compatilibilty of PDMS/glass with radiometals, the optimization of labeling conditions for NOTA/DOTA–(RGDfK) with radiometals using the microreactor, and comparisons between microfluidic and conventional radiosynthesis will be discussed in detail.

3.1. Compatibility of PDMS/glass with $^{68}Ga^{3+}$/$^{64}Cu^{2+}$:

One of the major problems with PDMS-based microreactor designed for radiosynthesis of ^{18}F-FDG is the loss of ^{18}F through reaction with (or absorption by) the PDMS. Therefore, the compatibility of the designed microreactor with radioisotopes is critical for its utilization in radiolabeling. In order to demonstrate the compatibility of our microreactor with ^{64}Cu, we have previously examined the retention of $^{64}Cu^{2+}$ and the ability of PDMS/glass to withstand the emissions of this radionuclide [31]. Here, we present additional data on compatibility of $^{68}Ga^{3+}$ with PDMS/glass-based reactors.

The retention studies of $^{68}Ga^{3+}$/$^{64}Cu^{2+}$ in a PDMS/glass micro-channel (Fig. 3) were performed in single microchannels (length =

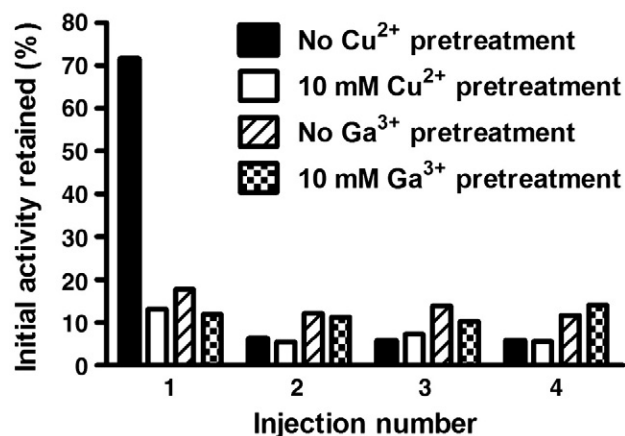**Fig. 3.** Retention of $^{68}Ga^{3+}/^{64}Cu^{2+}$ in a PDMS/glass microchannel.

3 cm, volume = 0.6 μL) with staggered herringbone grooves. Before the retention studies, the microchannels were washed with nitric acid to remove trace amounts of metal ions. The data shown in Fig. 3, clearly show that the non pre-treated microchannels retained a substantial portion of the activity of the first injection (~70%), but retained only ~5% of the activity of subsequent injections. The microchannel that was pre-treated with non-radioactive Cu^{2+} solution retained only ~15% of the activity of the first injection and also retained only ~5% of the activity of subsequent injections. The activity retention of subsequent injections decreased to around 5% for both pretreated and non-pretreated microchannels. The retention of $^{64}Cu^{2+}$ on microchannel was hypothesized to be due to the non-specific electrostatic interactions between $^{64}Cu^{2+}$ and the microchannel surface, and this hypothesis is consistent with the observation that pretreatment with Na^+ decreases the $^{64}Cu^{2+}$ retention similar to pretreatment with non-radioactive Cu^{2+}(data not shown) [31].

Interestingly, very little difference in the $^{68}Ga^{3+}$ retention (~15%) between the gallium-pretreated and untreated microchannels was observed, and no changes were evident after the microchannel was pre-treated with Na^+ solution (data not shown). To determine whether the buffer influences the retention of $^{64}Cu^{2+}/^{68}Ga^{3+}$, $^{64}Cu^{2+}$ stock solution was prepared in HEPES buffer (pH = 4.50) following the procedure for preparation of $^{68}Ga^{3+}$ stock solution (refer to *experimental section*). We observed that $^{64}Cu^{2+}$ retention performance in HEPES buffer (pH = 4.50) is similar to that in NH_4OAc buffer (pH = 6.50). Compared with $^{68}Ga^{3+}$, $^{64}Cu^{2+}$ has a much higher retention in the PDMS/glass microchannel in both two buffers, which indicates that the non-specific electrostatic interactions between gallium and PDMS/glass is very weak.

The PDMS-based microfluidic chip has withstood 260 mCi of radiometal and more than 720 h of radiation exposure, and has shown no sign of degradation or loss of function. The only observed sign of damage with the microreactor, which has been used for six months, is leakage caused by mechanical failure of the seal between the PDMS and glass. Based on this delayed observation of failure and the preceding results on retention, we conclude that the microreactor is compatible with $^{68}Ga^{3+}/^{64}Cu^{2+}$, and the interaction between the microreactor and $^{64}Cu^{2+}$ can be minimized by saturating the walls of the microchannels with cations. Thus, the microreactor is sufficiently robust and reliable for its envisioned role as a single or multiple use for radiometal labeling under aqueous condition.

3.2. Microfluidic radiolabeling of NOTA/DOTA−(RGDfK):

A variety of radiometal labeled *cyclo*(RGDfK) peptides have been used to monitor expression of the $\alpha_v\beta_3$ receptor, which is an integrin

required for tumor-induced angiogenesis, and very promising results were obtained [3–6]. The radiometal labeling of cylco(RGDfK) was conducted following the procedure described in the *Experimental section*. The labeling results were analyzed by radio-HPLC and/or radio-TLC(iTLC), and various TLC/iTLC developing solvents were used in order to obtain the best separation. The radiolabeling conditions were optimized by varying the reaction temperatures, concentrations and residence times, and the labeling results obtained using the microreactor were directly compared with those achieved *via* conventional radiosynthesis.

When radio-TLC was used to monitor the ^{64}Cu incorporation yield obtained after a short residence time (0.5 min), two complex isomers were observed for commonly used chelates, such as Cyclen, Cyclam, DOTA and TETA (data not shown). However, once the residence time was prolonged to 5 min or longer, the appearance of one of the isomers was totally eliminated. We speculate that these isomers are probably the ^{64}Cu bound intermediate, which undergoes further rearrangement to form the final complex with stable conformation. In the case of ^{64}Cu-NOTA-RGD, the ratio of the two complex isomers (R_f on developed TLC were 0.46, 0.53 respectively) did not change much even after the residence time was prolonged from 2 to 20 min, although the total incorporation yield was significantly increased. Regardless of the changes in ligand to metal ratio, reactant concentration and reaction temperature, only very small variations were observed in the ratios of the two isomers formed from ^{64}Cu-NOTA-RGD when comparing the conventional method and the microfluidic approach, which suggests that both the isomers are stable and may have adopted different geometrical configurations due to the bulky *p*-NH_2 benzyl substituent in NOTA chelator. These observations are consistent with recent reports using the same or similar radioligands [36]. Further investigation on how to produce a radiolabeled complex with a desired geometrical configuration is currently under progress, because different complex isomers may have different biological properties and applications *in vitro* and *in vivo*.

To optimize the labeling conditions using the microreactor, we first performed experiments with a fixed ligand to metal ratio (1:1), residence time (10 min) and incubation temperature (37 °C). The final concentration of radiometal, identical to the concentration of the ligand, was varied from 1 μM to 200 μM by adjusting both, the stock solutions and buffer-to-metal molar ratio, as previously described in the *Experimental section*. As shown in Fig. 4, with increasing final concentrations of carrier-added $^{64}Cu^{2+}/^{68}Ga^{3+}$, the reaction yields also increased dramatically from less than 10% with a final concentration of 1 μM to more than 90% with a final concentration of 90 μM. This increase is consistent with classical collision theory in that
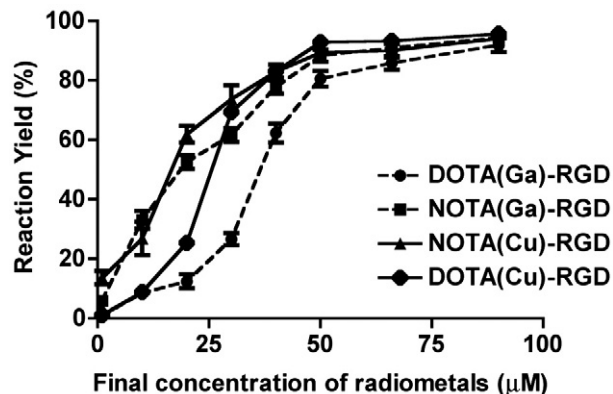

Fig. 4. Radiolabeling yields as a function of the final concentration of carrier-added $^{64}Cu^{2+}/^{68}Ga^{3+}$ on the microreactor using a 1: 1 stoichiometric ratio of radiometal to DOTA/NOTA-cyclo(RGDfK). Error bars represent standard deviation in the extent of reaction for three experiments (residence time = 10 min, T = 37 °C), using radiometal solutions made from the same batch of $^{64}Cu^{2+}/^{68}Ga^{3+}$.

reaction rates (as well as reaction yields for a given period of time) generally increases with increasing concentrations in the reaction mixtures. In conventional radiosynthesis with 1: 1 ligand to metal ratio, the final concentration of radiometal is typically less than 1 μM (20 mCi ≈ 85 picomoles of ^{64}Cu or 100 mCi ≈ 100 picomoles of ^{68}Ga in 100 μL reaction mixture), which will result in low labeling yields at a 1:1 stoichiometric ratio. In addition, trace metal impurities found in the radiometal adversely affects the labeling yield. Only very low labeling yields (<2%) could be obtained in such a short reaction time. Therefore, a large excess of ligands is usually employed in conventional radiosynthesis to compensate for dilution effects and metal impurities. Microfluidic approaches can alleviate the issues associated with dilution of cyclotron/generator produced radiometals by (1) using small volumes of concentrated radiometal, ligand and buffer solutions, and (2) implementing a microfluidic means to concentrate the reactants on-chip, such as evaporation of reaction solvent.

To study the effect of residence time, the labeling reactions were conducted by mixing 100 μM carrier-added $^{64}Cu^{2+}/^{68}Ga^{3+}$ solution and 100 μM DOTA/NOTA-RGD solution at a 1 : 1 stoichiometric ratio (100 μM concentration provided maximum yield) at 37 °C for different residence times (5 min, 10 min and 20 min); the data are summarized in Fig. 5A. Under these labeling conditions, at least a 10% increase in radiolabeling yield was observed for all four complexes when the residence time was prolonged from 5 min to 10 min. However, when the residence time was further extended, the increases in radiolabeling yields were relatively smaller compared

to the increases obtained from 5 to 10 min. These observations were expected, since the use of longer residence times leads to better radiolabeling yields, because both reactants have longer reaction times in the reservoirs before elution from the system. As time elapses, the amounts of available reactants are reduced along with the formation of the complexes, and the reaction rates increase at a slower rate and finally reach a plateau.

To study the effect of temperature, we used a radiometal concentration of 100 μM (based on Fig. 4), and residence time of 10 min (based on Fig. 5A), but varied the temperature. Fig. 5B shows radiolabeling yields obtained from the chelation reactions between carrier-added radiometals and the corresponding BFC-BMs (NOTA/ DOTA-RGD) at different temperatures (23, 37 and 47 °C). At room temperature (23 °C), moderate labeling yields (55%–75%) were obtained, except in the case of ^{68}Ga radiolabeling of DOTA-RGD (≤2.0%). When the temperature was increased, higher labeling yields (80%–90%) were observed at 37 °C and 47 °C. The increase in labeling yield with temperature is due to the fact that the energy activation barrier is lowered for the reaction at higher temperatures, which leads to improved reaction kinetics. Especially in the case of ^{68}Ga labeling of DOTA-RGD, a significant improvement in labeling yield (from ≤2.0% to 80%) is obtained since it is a very temperature sensitive reaction [4,37].

To demonstrate the advantages of enhanced mass and heat transfer at the microscale, we compared the labeling performance obtained using the microreactor and conventional methods with carrier-added radiometals (containing over 99% non-radioactive copper/gallium, referred to as radiometal solutions). The efficient mixing by staggered herringbone grooves enables effective handling of small reagent volumes. The enhanced heat transfer due to shorter path lengths will lead to the improved incorporation yields of the radiolabeling reactions. To compare the performance obtained using microreactor and conventional methods, we used a radiometal concentration of 100 μM (based on Fig. 4), a residence time of 10 min (based on Fig. 5A), and a temperature of 37 °C (Fig. 5B). These parameters were chosen, because under these conditions labeling yields were very high but not maximum, so there was still room to observe changes in performance.

The comparison of radiolabeling yields at different temperatures between microfluidics and conventional radiosynthesis for ^{68}Ga-DOTA-RGD is shown in Fig. 6A, while the comparison for all four labeling reactions under above-mentioned conditions is shown in Fig. 6B. For radiolabeling of DOTA-RGD with carrier-added $^{68}Ga^{3+}$, the most temperature sensitive reaction of all the four reactions, the yields were greatly improved when the temperatures were increased using either method, but microreactor-based labeling led to a much larger enhancement in the radiolabeling yields than conventional labeling at elevated temperature (37 and 47 °C), which validates the hypothesis of enhanced heat transfer at the microscale. For all four reactions, the labeling yields obtained using the microreactor were higher than those obtained using conventional methods, due to improved heat and mass transfer (Fig. 6B).

3.3. Preparation of no carrier-added radiometal-labeled BFC-BM:

All the above radiometal labeling experiments have been performed with carrier-added radiometals. The labeling with carrier-added radiometal is different from the labeling with no-carrier added radiometal, because the total amount of metal impurities in the latter case is typically high, in most cases even higher than the amount of radiometal of interest [38]. For clinical and pre-clinical applications, typically no-carrier added radiometal solutions are used. To validate the performance of the microreactor for these applications, no-carrier added radiometal labeled BFC-BMs were prepared. The four previously used radioligands (using no-carrier added radiometals), DOTA(^{64}Cu)-RGD, DOTA(^{68}Ga)-RGD, NOTA(^{64}Cu)-RGD and DOTA
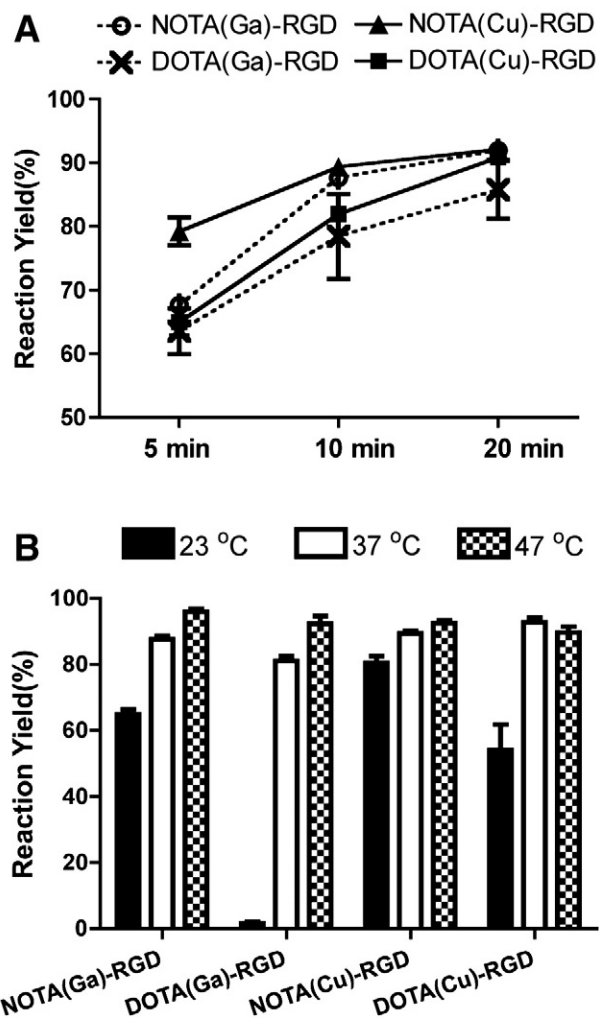

Fig. 5. Effect of (A) residence time, and (B) temperature on the labeling of DOTA/NOTA-cyclo(RGDfK) with carrier-added $^{64}Cu^{2+}/^{68}Ga^{3+}$.
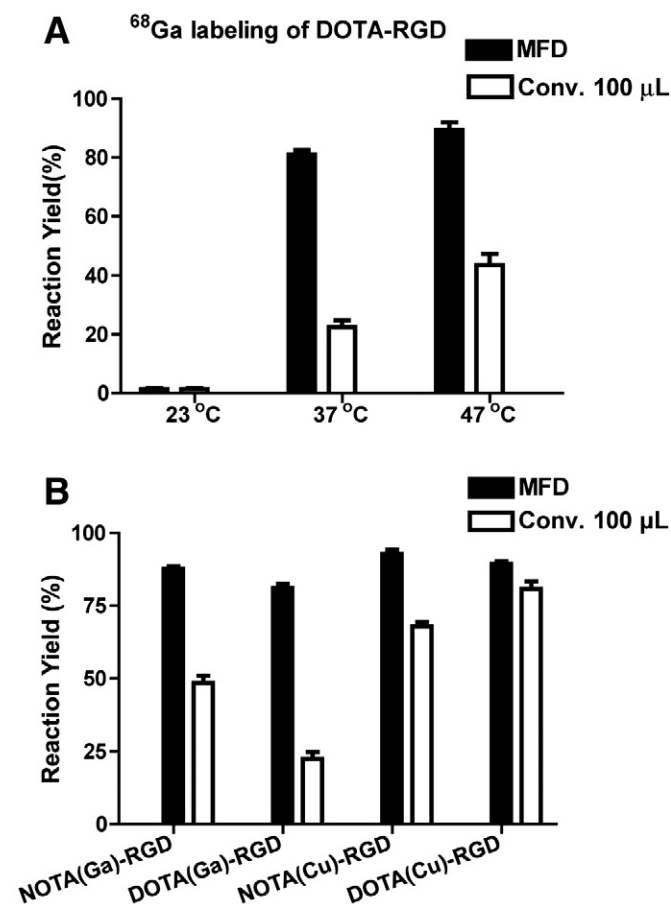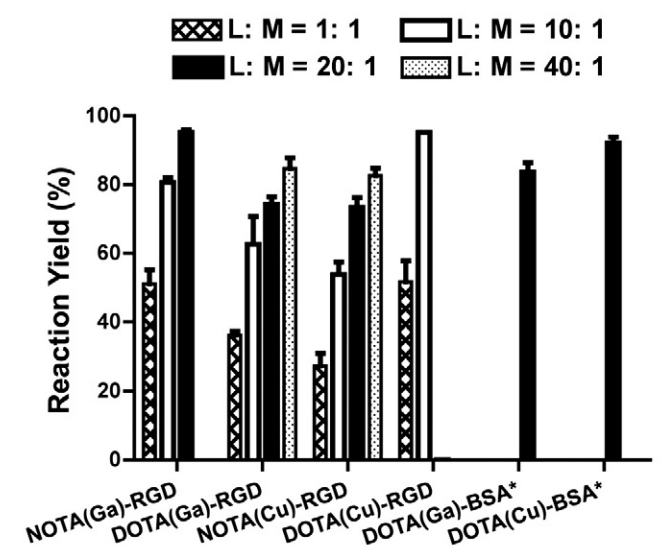
Fig. 6. Comparison of radiolabeling results between two approaches, microreactor and conventional method: (A) labeling DOTA-RGD with carrier-added $^{68}Ga^{3+}$ at different temperature (23, 37 and 47 °C) with a residence time of 10 min; (B) labeling NOTA/DOTA-RGD with carrier-added $^{64}Cu^{2+}/^{68}Ga^{3+}$ with a residence time of 10 min at 37 °C.

(^{68}Ga)-RGD were prepared by using a microreactor under the optimized conditions described in the previous section (at 37 °C, and a residence time of 10 min, while the concentration of radiometals

Fig. 7. Preparation of no-carrier added $^{64}Cu^{2+}/^{68}Ga^{3+}$ labeled BFC-BM with different L:M ratio at 37 °C, and a residence time of 10 min for DOTA/NOTA-RGD peptides and a residence time of 20 min for DOTA-BSA proteins.
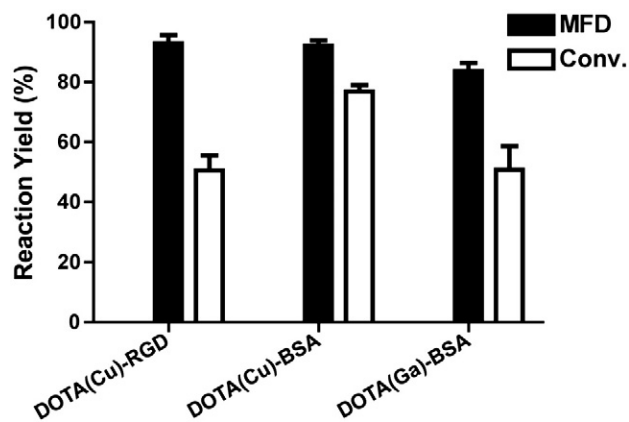

Fig. 8. Direct comparison of the labeling yields obtained from two approaches, microreactor and conventional methods under identical conditions: 37 °C; L:M = 20: 1; and a residence time of 10 min for DOTA/NOTA-RGD peptides and a residence time of 20 min for DOTA-BSA proteins.

varied from batch to batch: [^{64}Cu] = 3–5 μM ; [^{68}Ga] = 5–8 μM). In addition to RGD, we also studied labeling of DOTA-BSA, as a representative protein for larger macro-biomolecules (proteins and antibodies). The purpose for labeling BSA was to evaluate the microreactor's ability to label large molecules compared to peptides (smaller molecules), since larger molecules may mix slower due to lower diffusivity.

The results for these no-carrier added radiolabeling experiments are summarized in Fig. 7. For all reactions: (1) BFC-BM was successfully radiolabeled using microreactors at 37 °C in a relatively short time (with a residence time of 10 min for RGD peptide), except for the labeling of BSA, where the residence time was 20 min; (2) excess ligand was generally required for efficient radioisotope incorporation in such a short time and the radiolabeling yield increased with increasing L:M ratio. This increase in yield is due to higher concentration of BFC-BM and increased probability of chelation of the BFC-BM with the radiometal of interest. Note that the values of L: M ratio in Fig. 7 may not be accurate, as the concentrations of no-carrier added radiometal were estimated from the average effective specific activity. In addition, the labeling performance of DOTA-RGD peptide and DOTA-BSA protein with no-carrier added radiometal using microreactor and conventional methods (Fig. 8) was also compared. Again, the microfluidic approach greatly improved the radiolabeling yields compared to the yields obtained with conventional methods, similar to the carrier-added radiolabeling results reported above. Fig. 9 compares the calculated specific activities of the
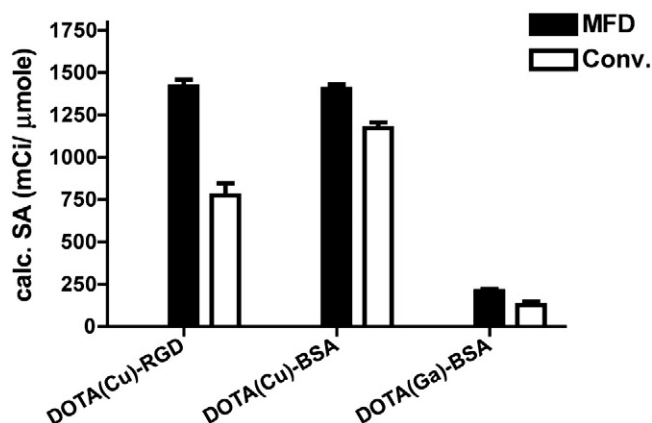

Fig. 9. Direct comparison of the calculated specific activities obtained from two approaches, microreactor and conventional for no-carrier added radiolabeling of DOTA(Cu)-RGD, DOTA(Cu)-BSA and DOTA(Ga)-BSA.

no-carrier added preparations of DOTA(Cu)-RGD, DOTA(Cu)-BSA and DOTA(Ga)-BSA based of the specific activities of the radiometals and the labeling yields. These no-carrier added labeling results suggest the tremendous potential of the microreactor for the preparation of radiopharmaceuticals in pre-clinical and/or clinical environments.

4. Conclusion

In summary, a robust, reliable, compact microreactor capable of chelating radiometals with common chelates has been developed and validated. The microreactor was used for the preparation of a variety of $^{64}Cu^{2+}/^{68}Ga^{3+}$ labeled BFC-BMs, in which the BM included both peptide and protein, and the BFC included two common ligands DOTA and NOTA. The radiolabeling conditions were optimized with carrier-added radiometals by varying the residence time, concentration and temperature, and comprehensive comparisons between microfluidic and conventional methods were conducted with both carrier-added and no-carrier added radiometals. Based on our radiolabeling results, the reported microfluidic approach overall outperforms conventional radiosynthetic methods, and is thus a promising technology for the radiometal labeling of commonly utilized BFC-BMs in aqueous solutions.

References

[1] Tanaka K, Fukase K. PET (positron emission tomography) imaging of biomolecules using metal-DOTA complexes: a new collaborative challenge by chemists, biologists, and physicians for future diagnostics and exploration of in vivo dynamics. Org Biomol Chem 2008;6:815-28.

[2] Auzzas L, Zanardi F, Battistini L, Burreddu P, Carta P, Rassu G, et al. Targeting alphavbeta3 integrin: design and applications of mono- and multifunctional RGD-based peptides and semipeptides. Curr Med Chem 2010;17:1255-99.

[3] Dijkgraaf I, Beer AJ, Wester HJ. Application of RGD-containing peptides as imaging probes for alphavbeta3 expression. Front Biosci 2009;14:887-99.

[4] Dumont RA, Hildebrandt I, Su H, Haubner R, Reischl G, Czernin JG, et al. Noninvasive imaging of alphaVbeta3 function as a predictor of the antimigratory and antiproliferative effects of dasatinib. Cancer Res 2009;69:3173-9.

[5] Cai W, Sam Gambhir S, Chen X. Multimodality tumor imaging targeting integrin alphavbeta3. Biotechniques 2005;39:S14-25.

[6] Haubner R. Alphavbeta3-integrin imaging: a new approach to characterise angiogenesis? Eur J Nucl Med Mol Imaging 2006;33(Suppl 1):54-63.

[7] Tian X, Chakrabarti A, Amirkhanov NV, Aruva MR, Zhang K, Mathew B, et al. External imaging of CCND1, MYC, and KRAS oncogene mRNAs with tumor-targeted radionuclide-PNA-peptide chimeras. Ann N Y Acad Sci 2005;1059:106-244.

[8] Green MA, Mathias CJ, Welch MJ, McGuire AH, Perry D, Fernandez-Rubio F, et al. Copper-62-labeled pyruvaldehyde bis(N4-methylthiosemicarbazonato)copper(II): synthesis and evaluation as a positron emission tomography tracer for cerebral and myocardial perfusion. J Nucl Med 1990;31:1989-96.

[9] Li WP, Lewis JS, Kim J, Bugaj JE, Johnson MA, Erion JL, et al. DOTA-D-Tyr(1)-octreotate: a somatostatin analogue for labeling with metal and halogen radionuclides for cancer imaging and therapy. Bioconjug Chem 2002;13:721-8.

[10] Leung K. 68 Ga-1,4,7-triazacyclononane,1-glutaric acid-4,7-acetic acid-cyclo(Arg-Gly-Asp-d-Phe-Lys). Bethesda (MD): Molecular Imaging and Contrast Agent Database (MICAD); 2004.

[11] Maecke HR, Hofmann M, Haberkorn U. (68)Ga-labeled peptides in tumor imaging. J Nucl Med 2005;46(Suppl 1):172S-8S.

[12] Velikyan I, Maecke H, Langstrom B. Convenient preparation of 68Ga-based PET-radiopharmaceuticals at room temperature. Bioconjug Chem 2008;19:569-73.

[13] Wadas TJ, Wong EH, Weisman GR, Anderson CJ. Coordinating radiometals of copper, gallium, indium, yttrium, and zirconium for PET and SPECT imaging of disease. Chem Rev 2010;110:2858-902.

[14] Ma D, Lu F, Overstreet T, Milenic DE, Brechbiel MW. Novel chelating agents for potential clinical applications of copper. Nucl Med Biol 2002;29:91–105.

[15] Connett JM, Buettner TL, Anderson CJ. Maximum tolerated dose and large tumor radioimmunotherapy studies of 64Cu-labeled monoclonal antibody 1A3 in a colon cancer model. Clin Cancer Res 1999;5:3207s-12s.

[16] Ehrhardt GJ, Welch MJ. A new germanium-63/gallium-68 generator. J Nucl Med 1978;19:925-9.

[17] Wadas TJ, Anderson CJ. Radiolabeling of TETA- and CB-TE2A-conjugated peptides with copper-64. Nat Protoc 2006;1:3062-8.

[18] Reichert DE, Hancock RD, Welch MJ. Molecular mechanics investigation of gadolinium(III) complexes. Inorg Chem 1996;35:7013-20.

[19] DeMello AJ. Control and detection of chemical reactions in microfluidic systems. Nature 2006;442:394-402.

[20] Watts P, Haswell SJ. The application of micro reactors for organic synthesis. Chem Soc Rev 2005;34:235-46.

[21] Jahnisch K, Hessel V, Lowe H, Baerns M. Chemistry in microstructured reactors. Angew Chem Int Ed Engl 2004;43:406-46.

[22] Ungersboeck J, Philippe C, Mien LK, Haeusler D, Shanab K, Lanzenberger R, et al. Microfluidic preparation of [18F]FE@SUPPY and [18F]FE@SUPPY:2—comparison with conventional radiosyntheses. Nucl Med Biol 2011;38:427-34.

[23] Gillies JM, Prenant C, Chimon GN, Smethurst GJ, Dekker BA, Zweit J. Microfluidic technology for PET radiochemistry. Appl Radiat Isot 2006;64:333-6.

[24] Audrain H. Positron emission tomography (PET) and microfluidic devices: a breakthrough on the microscale? Angew Chem Int Ed Engl 2007;46:1772-5.

[25] Miller PW, Long NJ, de Mello AJ, Vilar R, Passchier J, Gee A. Rapid formation of amides via carbonylative coupling reactions using a microfluidic device. Chem Commun 2006:546-8.

[26] Elizarov AM. Microreactors for radiopharmaceutical synthesis. Lab Chip 2009;9:1326-33.

[27] Liu K, Lepin EJ, Wang MW, Guo F, Lin WY, Chen YC, et al. Microfluidic-based 18F-labeling of biomolecules for immuno-positron emission tomography. Mol Imaging 2011;10(168–76):1-7.

[28] Lee CC, Sui G, Elizarov A, Shu CJ, Shin YS, Dooley AN, et al. Multistep synthesis of a radiolabeled imaging probe using integrated microfluidics. Science 2005;310:1793-6.

[29] Elizarov AM, van Dam RM, Shin YS, Kolb HC, Padgett HC, Stout D, et al. Design and optimization of coin-shaped microreactor chips for PET radiopharmaceutical synthesis. J Nucl Med 2010;51:282-7.

[30] Lu SY, Watts P, Chin FT, Hong J, Musachio JL, Briard E, et al. Syntheses of 11C- and 18F-labeled carboxylic esters within a hydrodynamically-driven micro-reactor. Lab Chip 2004;4:523-5.

[31] Wheeler TD, Zeng D, Desai AV, Onal B, Reichert DE, Kenis PJ. Microfluidic labeling of biomolecules with radiometals for use in nuclear medicine. Lab Chip 2010;10:3387-96.

[32] Stroock AD, Dertinger SK, Ajdari A, Mezic I, Stone HA, Whitesides GM. Chaotic mixer for microchannels. Science 2002;295:647-51.

[33] Sun X, Rossin R, Turner JL, Becker ML, Joralemon MJ, Welch MJ, et al. An assessment of the effects of shell cross-linked nanoparticle size, core composition, and surface PEGylation on in vivo biodistribution. Biomacromolecules 2005;6:2541-54.

[34] McCarthy DW, Shefer RE, Klinkowstein RE, Bass LA, Margeneau WH, Cutler CS, et al. Efficient production of high specific activity 64Cu using a biomedical cyclotron. Nucl Med Biol 1997;24:35-43.

[35] McCarthy DW, Bass LA, Cutler PD, Shefer RE, Klinkowstein RE, Herrero P, et al. High purity production and potential applications of copper-60 and copper-61. Nucl Med Biol 1999;26:351-8.

[36] Schlesinger J, Rajander J, Ihalainen JA, Ramesh D, Eklund P, Fagerholm V, et al. Isomerism of [64Cu-NOTA-Bn]-labeled radiotracers: separation of two complex isomers and determination of their interconversion energy barrier using ion pair chromatography. Inorg Chem 2011;50:4260-71.

[37] Ferreira CL, Lamsa E, Woods M, Duan Y, Fernando P, Bensimon C, et al. Evaluation of bifunctional chelates for the development of gallium-based radiopharmaceuticals. Bioconjug Chem 2010;21:531-6.

[38] Carey P, Liu Y, Kume M, Lapi S, Welch M. The production of high specific activity Cu-64 as measured by ion chromatography. J Nucl Med Meeting Abstracts 2010;51:1552.